PROCEEDINGS B

royalsocietypublishing.org/journal/rspb

Research

Cite this article: Wu D *et al*. 2025 Earth history and trait innovation drive the global radiation of modern toads. *Proc. R. Soc. B* **292**: 20251928.
https://doi.org/10.1098/rspb.2025.1928

Received: 30 July 2025
Accepted: 4 September 2025

Subject Category:
Evolution

Subject Areas:
evolution, systems biology, taxonomy and systematics

Keywords:
Bufonidae, biogeography, phenotypic innovation, Earth history, long-distance dispersal

Authors for correspondence:
Zhiyong Yuan
e-mail: yuanzhiyongkiz@126.com
Wei Xu
e-mail: xuwei.evo@gmail.com

Electronic supplementary material is available online at https://doi.org/10.6084/m9.figshare.c.8054263.

Earth history and trait innovation drive the global radiation of modern toads

Dongyi Wu[1], Elizabeth Prendini[2], Christopher J. Raxworthy[2], Zhijian Wang[1], Weiwei Zhou[3], Jinmin Chen[4], Chatmongkon Suwannapoom[5], Phuping Sucharitakul[6], Marcio R. Pie[7,8], Wei Xu[9] and Zhiyong Yuan[1]

[1]Key Laboratory of Freshwater Fish Reproduction and Development (Ministry of Education), Integrative Science Center of Germplasm Creation in Western China (Chongqing) Science City, Chongqing Innovation Center for Biotechnology in Breeding, School of Life Sciences, Southwest University, Chongqing 400715, People's Republic of China
[2]Department of Herpetology, American Museum of Natural History, New York 10024, USA
[3]State Key Laboratory of Herbage Improvement and Grassland Agro-ecosystems, and College of Ecology, Lanzhou University, Lanzhou 730000, People's Republic of China
[4]Anhui Provincial Key Laboratory of the Conservation and Exploitation of Biological Resources, College of Life Sciences, Anhui Normal University, Anhui 241000, People's Republic of China
[5]School of Agriculture and Natural Resources, University of Phayao, Phayao 56000, Thailand
[6]School of Environment, Tsinghua University, Beijing 100084, People's Republic of China
[7]Ecology Biology Department, Edge Hill University, Lancashire L39 4QP, UK
[8]Departamento de Zoologia, Universidade Federal do Paraná, Curitiba, Paraná, Brazil
[9]DIADE, Université Montpellier, CIRAD, IRD, Montpellier 34394, France

CJR, 0000-0002-4517-0447; JC, 0000-0001-6432-7721; MRP, 0000-0002-2949-4871; WX, 0000-0002-4184-3982; ZY, 0000-0001-5991-3021

The distributions of species radiations reflect environmental changes driven by both Earth history (geological processes) and the evolution of biological traits (critical to survival and adaptation), which profoundly drive biodiversity yet are rarely studied together. Modern toads (Bufonidae, Amphibia), an iconic radiation with global distribution and high phenotypic diversity, are an ideal group for exploring these dynamics. Using phylogenomic data from 124 species across six continents, we reconstruct their evolutionary history. Biogeographic analyses suggest modern toads originated in South America approximately 61 million years ago (Ma), later dispersing to Africa and Asia, thereby challenging hypotheses of dispersal via North America. Species diversification rates increased after leaving South America, linked to Cenozoic geological events and key innovations like toxic parotoid glands for predator defence. The emergence of parotoid glands coincided with the South American dispersal, promoting diversification and enabling toads to dominate both Old and New Worlds. In contrast, the evolution of other traits, despite being crucial to adaptation, did not promote species diversification (e.g. large body size) or were ambiguously associated with expansion into the Old World (e.g. developmental modes). These findings highlight the adaptability of modern toads and reveal the interplay between Earth's history and phenotypic innovation in shaping biodiversity.

1. Introduction

One of the central goals of biogeography is to uncover the patterns and processes shaping the distribution of biodiversity across the planet [1,2]. These patterns reveal fascinating contrasts, such as the distinct evolutionary legacies of species that once thrived on the ancient supercontinents of Gondwana and Laurasia [3,4], the dramatic divide in species composition between Southeast Asia and Australia, marked by the famous Wallace Line

THE ROYAL SOCIETY PUBLISHING

[5,6], and the striking diversity gradient stretching from the temperate North American to the species-rich ecosystems of South America, driven by the Great America Biotic Interchange facilitated by the formation of the Isthmus of Panama [7–9]. Each of these examples reflects the intricate interplay of Earth's geological history, climatic changes and evolutionary processes, which together have shaped the complex patterns of biodiversity observed across the globe today [10–12].

Geological processes, particularly the tectonic breakup and reassembly of continents, have played a pivotal role in driving vicariance, dispersal and regional diversification [13,14]. Early-diverging lineages, once broadly distributed across continents, were often isolated by plate tectonics. In contrast, more recent lineages expanded their range via land bridges or island chains formed through tectonic activity or climatic shifts, promoting diversification in newly accessible regions. These processes have been linked to the continental distribution patterns observed in various groups, including plants [13,15], birds [16], amphibians [17,18] and fishes [19], particularly in taxa with limited dispersal capabilities.

Trait evolution shapes species distribution patterns through its interplay with species diversification or dispersal [20]. Group-specific key innovations (e.g. wings of birds, a classical example) can drive both rapid adaptation and colonization to diverse environments, thereby influencing species' geographic distribution [21,22].

While both geological history and trait evolution are widely recognized as major drivers of species distributions, they are often studied in isolation. This leaves a key question unanswered: how do Earth's geological history and trait evolution jointly shape global biodiversity patterns?

Modern toads (Bufonidae, Amphibia) are well known for their global success in colonizing diverse environments, making them an ideal model to bridge the gap in understanding biodiversity patterns due to their remarkable diversity and trait variation on a global scale [23–25]. Toads are notorious for their strong invasive capacity, originally absent only in Antarctica, Australia (except for the invasive species *Rhinella marina* [26]), Madagascar (recently invaded by *Duttaphrynus melanostictus* [27]) and the Mascarene Islands (Mauritius, La Réunion), where *Sclerophrys gutturalis* is now invasive [28]. With 52 genera and 648 extant species [29], modern toads are one of the most species-rich amphibian groups, occupying diverse ecological niches including terrestrial, arboreal and burrowing habitats [30]. They also serve as key biological models in fields such as invasive biology (e.g. the cane toad, *Rhinella marina* [26]), evolutionary biology (e.g. the Chinese toad, *Bufo gargarizans* [31]) and developmental biology (e.g. the common toad, *Bufo bufo* [32]).

Despite their importance in many biological investigations, the evolutionary history of modern toads remains elusive. Recent evidence supports a South American origin—first proposed by Blair [33]—as both basal lineages and outgroups are found in this region [24,34,35]. These findings refute earlier hypotheses proposing an African [36] or a broader Gondwanan origin [37]. However, considerable uncertainty persists regarding the timing of their origin and the pathways of their subsequent intercontinental expansion—particularly concerning the routes from New World to the Old World [24,30,34,35]. Several hypotheses have been proposed. The 'Trans-Pacific colonization route', first suggested by Blair [33] and later supported by Pramuk *et al.* [34], posits a northward expansion from South America into Central and North America, followed by dispersal into Asia via the Bering land bridge. However, this scenario suffers from limited sampling of Asian taxa, resulting in incomplete phylogenies. Pramuk *et al.* [34] also proposed the possibility of a 'Trans-Atlantic colonization route', involving dispersal via the North Atlantic land bridge, but ultimately favoured the Bering pathway based on the available phylogeny and without formal testing methods. Notably, they only considered the Trans-Atlantic route as a possible path for secondary re-invasion from the Old World back into the New World, rather than an initial colonization route.

These land bridge-based scenarios have been widely accepted, either implicitly or explicitly, in earlier studies and are commonly invoked across many other taxa [13,38]. For amphibians like toads—characterized by limited saltwater tolerance and low dispersal ability—such land connections have often been viewed as the most plausible explanation for intercontinental dispersal. A more recent and less conventional hypothesis, proposed by Pyron [35], suggests a 'Trans-Atlantic oceanic colonization route' from South America to Africa, without the involvement of land bridges. However, the limited genetic sampling in this large-scale amphibian phylogeny resulted in poorly resolved relationships among American and African lineages, hindering a robust evaluation of this scenario. Van Bocxlaer *et al.* [24] did not clearly favour any particular dispersal route, but they were the first to link the global radiation of toads with the emergence of key morphological traits—such as increased body size and the development of parotoid glands—which may have facilitated ecological and geographic expansion. However, they did not analyse the evolutionary dynamics of these traits or their potential association with diversification rates, leaving such interpretations speculative and based largely on temporal coincidence.

Addressing these gaps in species sampling, phylogenetic resolution and trait-based diversification analyses is therefore critical to fully understanding the processes that enabled toads to achieve their present-day global distribution. Here, we generate a well-resolved species-level phylogeny for modern toads using a probe-capture-based phylogenomic dataset and compile a comprehensive trait dataset to uncover their spatiotemporal evolutionary processes across major continents. This phylogeny encompasses 70.4% of extant species, integrating data from previous studies and representing all major clades. We selected five traits (body size, parotoid glands, inguinal fat bodies, adult habitat types, developmental modes) from Van Bocxlaer *et al.* [24], as these are hypothesized to play crucial roles in various aspects of toad natural history, including survival, adaptation and global expansion. Our study aims to address two key questions: (i) by which routes did modern toads colonize the world, and how were these influenced by geological history? And (ii) how did trait evolution influence diversification and distribution patterns during global expansion?

2. Material and methods

(a) Novel taxon sampling and probe design

To construct a well-resolved phylogeny of Bufonidae, we generated a phylogenomic dataset using anchored hybridization enrichment (AHE) [39]. The loci are homologous to the AHE loci developed by Lemmon *et al.* [39] and applied in Hime *et al.* [40]. To obtain the gene sequences across Bufonidae, we mined 220 amphibian-specific orthologous AHE loci from the whole genome of *Bufo bufo* (GCA_905171765.1). Among these, 219 conserved orthologous genes were identified, and a probe set was designed to target these loci. To integrate AHE data with existing mitochondrial sequences from previous studies (see below), we selected 13 mitochondrial genes for probe design, based on the mitochondrial genome of *Bufo gargarizans* (NC_008410.1). We designed a set of 100-mer DNA probes tiled across each of these loci, with different numbers of probes designed according to the length of each gene. The tiling density of probes over target regions ranged from 3 to 4. A total of 9807 biotinylated 100-mer RNA probes were designed, and the region covered by the probes was approximately 933 bp per locus on average. The probes were synthesized by iGeneTech Bioscience Co., Ltd. (Beijing, China).

We sampled 124 species representing all major Bufonidae clades, referencing prior studies [24,30,34,35], for AHE sequencing using the probes designed above. In addition, drawing on previous large-scale phylogenetic studies on amphibians [17,40,41], we included seven species as outgroups. AHE nuclear loci for six outgroups were obtained from Hime *et al.* [40], and *Hyla annectans* (Hylidae) were newly sequenced. Detailed sampling information of the AHE dataset is provided in electronic supplementary material, table S1.

(b) DNA extractions, library preparation and sequencing

We extracted genomic DNA from tissues using the Qiagen DNAeasy Tissue Extraction Kits (QIAGEN, Valencia, CA). We followed the Hyb-Seq method of Mandel *et al.* [42], with library construction, capture preparation and sequencing performed by iGeneTech Bioscience Co., Ltd. (Beijing, China). In brief, 200 ng of genomic DNA of each individual was sheared by Biorupter (Diagenode, Belgium) to acquire 150–200 bp fragments. The ends of the DNA fragments were repaired and affixed with an Illumina adapter (Fast Library Prep Kit, iGeneTech, Beijing, China). After the library construction, the samples were pooled (8–12 samples per batch) for multiplexed target capture using the 9807 custom-designed probes. Based on these probes, captured libraries were obtained, mixed in equal molar amounts and sequenced on the Illumina platform (Illumina, San Diego, CA) with 150 base paired-end reads.

The quality of the demultiplexed raw paired-end sequenced reads was assessed using FastQC v0.12.0 (https://www.bioinformatics.babraham.ac.uk/projects/fastqc/). We processed the reads using Trimmomatic v0.39 [43] to produce a cleaned dataset. This involved trimming Illumina adapters, removing reads below the defined quality threshold (sliding-window set to 5 : 20), and discarding short-cleaned reads (<50 bp length) or reads missing forward or reverse pairs. Cleaned reads were assembled with HybPiper v2.0.1 [44]. The reads were first mapped to the targets using BWA v0.7.17 [45] and then assembled into contigs using SPAdes v3.15.4 [46]. We aligned the FASTA files using Mafft v7.226 [47], trimmed the resulting alignments using the default settings in trimAl v14 [48], removed ambiguously aligned positions, and then manually checked each FASTA file. In total, we obtained 155 high-quality gene sequences from the samples, comprising 150 nuclear loci and 5 mitochondrial loci. All aligned sequences were concatenated into one sequence set for downstream analyses. The AHE sequence data are available on Dryad.

(c) Inclusion of existing sequence data

To maximize species sampling, we conducted a comprehensive review of systematic studies on modern toads (up to January 2023) focusing on 'molecular phylogeny', to ensure that a large amount of existing Sanger sequence data was included in our phylogenetic analyses. We identified 73 relevant articles published between 1997 and 2023 (electronic supplementary material, S1) and manually reviewed each. From these studies, we extracted sequence data for the corresponding species while taking precautions to minimize species identification errors, which are common in GenBank records. In total, we compiled sequences for 13 widely used molecular markers in amphibian phylogenetics [41,49,50]. These included seven nuclear genes (*NCX1*, *CXCR4*, *POMC*, *RAG1*, *H3A*, *RHOD*, *SLC8A1*) and six mitochondrial genes (12S rRNA, 16S rRNA, *ND1*, *ND2*, *CYTB*, *CO1*) from 332 species (GenBank accessions can be found in electronic supplementary material, S1). Of these, five mitochondrial genes (16S rRNA, *ND1*, *ND2*, *CYTB*, *CO1*) overlapped with the AHE dataset. In total, the combined AHE and published dataset included 456 species, accounting for 70.4% of all species of Bufonidae.

(d) Phylogenetic inference

We constructed phylogenies using both the AHE dataset alone and the concatenated dataset incorporating published sequences (hereafter referred to as the 'combined dataset'), applying the same workflow for both. Each locus was partitioned by codon position, with non-protein coding genes, such as 12S rRNA and 16S rRNA, treated as single partitions. The maximum likelihood (ML) tree was estimated using RAxML v8.2.11 [51] with the GTRGAMMA model assigned to each partition. Node support was assessed using rapid bootstrap analysis (option—f a) with 1000 replicates. In addition, we performed partitioned rapid bootstrapping to generate 100 bootstrap trees with branch length (option—k) for evaluating branch support.

To account for varying coalescent histories across loci, we estimated the species tree using ASTRAL v5.7.8 [52]. We ran ASTRAL using only the best ML tree from each of the 150 nuclear loci to avoid potential effects from sequence variability. ASTRAL produced trees with branch support values derived from local posterior probabilities [53]. All alignments and trees are available on Dryad.

(e) Divergence time analyses

Given the consistent topology observed across different datasets and approaches (see section Results in electronic supplementary material, figures S2–S4), we selected the combined dataset for subsequent analyses to maximize species representation. We conducted divergence-time estimation using penalized likelihood [54] implemented in treePL [55] on the best tree of RAxML. This method has been widely used for dating phylogenies with large numbers of species. We began by reviewing calibration points from recent amphibian studies [17,40,49] and selected five calibration points to calibrate the phylogeny (electronic supplementary material, table S2). Given the lack of sufficient evidence to confirm that the Paleocene '*Bufo*' from Brazil represents the oldest true *Bufo* species [56], this fossil was conservatively employed to calibrate the origin of Hyloidea. To identify the appropriate level of rate heterogeneity in the phylogram, we tested cross-validation with standard smoothing values from 10^{-10} to 10^{6} in treePL. The optimal smoothing value was determined based on the lowest χ^2 value. The best-fit smoothing parameter was 10^{-5}. We generated confidence intervals by running treePL 100 iterations on the best tree of RAxML, using the same smoothing value, to produce 100 time-calibrated trees to account for the uncertainty associated with penalized likelihood estimation. The time tree with confidence intervals was generated using TreeAnnotator v1.10.4 [57]. All the time trees are available on Dryad.

(f) Biogeographic reconstruction

To test alternative hypotheses on the intercontinental dispersal of modern toads, we developed a series of biogeographic models representing different colonization routes between major continents in the New World and the Old World. These included ten structured scenarios built around three major hypotheses (M1–M3; figure 1), alongside a null model (M0) assuming equal dispersal among regions (see electronic supplementary material, Methods). Detailed model descriptions are provided in electronic supplementary material, Methods.

To infer the optimal biogeographic scenario, a model-testing approach was applied using the R package BioGeoBEARS v0.2.1 [58] based on the tree generated by treePL, excluding outgroups. Following previous biogeographic analyses on modern toads [24,34,35,59,60] and the current distribution pattern [29], we defined six biogeographic regions corresponding to their global distribution: South America, Central America, North America, Africa, Asia and Europe (figure 1), as the spatial units for our biogeographic analyses. These six regions capture well-supported phylogeographic breaks that correspond to major historical dispersal events and vicariant barriers in the evolutionary history of modern toads [34,59]. Furthermore, these regions broadly correspond to those recognized in global amphibian biogeographic reconstructions and are consistent with area units used in major analyses of anuran global dispersal [35]. Geographical distribution data for each species were compiled from AmphibiaWeb (electronic supplementary material, table S3, [29]). Analyses were conducted using six models implemented in BioGeoBEARS: Dispersal-Extinction Cladogenesis (DEC [61]), the ML version of Dispersal Vicariance Analysis (DIVALIKE [62]), the Bayesian biogeographical inference model (BAYAREALIKE [63]) and their extension with a founder-event speciation parameter (+J). Different dispersal matrices were used to limit the dispersal among regions according to the ten possible scenarios (figure 1; electronic supplementary material, table S4). We set the value of free dispersal between two regions to 1, and the value of strictly restricted dispersal to 0.001 (electronic supplementary material, table S4). All analyses set the maximum possible distribution of ancestor nodes to two. Model fits were evaluated using AIC and relative model weights.

(g) Species diversification analyses

We investigated changes in diversification rates over time by estimating diversification dynamics using the Bayesian analysis of macroevolutionary mixtures (BAMM v2.5.0 [64]). The time tree, excluding outgroups, was used as the input tree. Priors were configured using the R package BAMMtools v2.1.10 [65]. To account for incomplete taxon sampling, sampling fraction data for each genus-level clade were provided (electronic supplementary material, table S5). The BAMM analysis was run for 10 million generations at a temperature-increment parameter of 0.01 and sampled event data every 1000 generations. The first 30% of samples were removed as burn-in. Effective sampling size (ESS) values were examined using the R package coda [66]. The post-burn-in output files were analysed using BAMMtools by assessing posterior probabilities for the selected best rate-shift configuration and the 95% credible rate shift configuration. Rate-through-time curves, including speciation (λ), extinction (μ) and net diversification (r), were summarized and visualized under the best shift model using BAMMtools. To complement the molecular evidence with data from extinct species, we also reconstructed extinction dynamics based on fossil records of Bufonidae retrieved from the Paleobiology Database (PBDB; paleobiodb.org/). Fossil-based diversification analyses were conducted using a Bayesian framework implemented in PyRate [67,68]. Detailed procedures and parameter settings for PyRate analyses are described in electronic supplementary material, Methods.

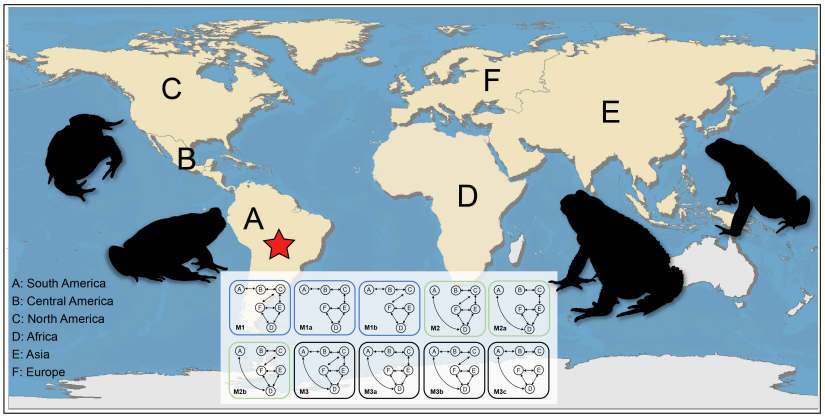

Figure 1. The map highlights six major biogeographic regions: South America (A), Central America (B), North America (C), Africa (D), Asia (E)nd Europe (F). The red star indicates the approximate origin of Bufonidae in South America. The white panel illustrates ten possible dispersal routes originating from South America (A), with arrows indicating dispersal direction. These models are categorized into three main types: (M1) northward expansion and land-bridge-connected dispersal, (M2) Trans-Atlantic long-distance dispersal and (M3) mixed-mode dispersal from South America to both North America and Africa. Toad silhouettes sourced from PhyloPi (https://www.phylopic.org/images).

(h) Trait-dependent diversification analyses

To characterize the trait evolution of modern toads, we compiled a species-level dataset encompassing five traits that present key aspects of their life history, including body size, adult habitat types, developmental modes and important organs such as parotoid glands and inguinal fat bodies (electronic supplementary material, S2). Data were coded following Van Bocxlaer *et al.* [24] and updated using the recent International Union for Conservation of Nature (IUCN) global amphibian assessment [69], AmphibiaWeb [29], and published literature (see details in electronic supplementary material, S2). We visualized the species composition distribution of all five traits across major continents in a world map. All the trait data used in this study were categorical characters.

Ancestral state reconstruction was performed for each trait to obtain the origin ages of each state. We used stochastic character mapping of discrete traits via SIMMAP [70] using the R package phytools v2.0.3 [71]. The best-fit model of character evolution was determined by fitting an equal-rates model and an all-rates-different (ARD) model to the dataset using the function 'fitDiscrete' in Geiger v2.0.6 [72]. Model fit was compared using the AICc [73]. The ARD model had the best fit to most of the data, followed by SYM (electronic supplementary material, table S6). We simulated 1000 stochastic character maps from the dataset using the ARD model and obtained posterior probabilities for the nodes by averaging the state frequencies across all maps. Reconstructions were conducted on the treePL time tree. For the reconstruction of each trait, the time tree was pruned to include only the species for which that trait was available.

To estimate rates of speciation and extinction associated with each state of a trait, we applied the Several Examined and Concealed States-dependent Speciation and Extinction models from the R package SecSSE v2.1.746 [74] to account for the variation within each observed state by including the hidden states. Following Liedtke *et al.* [75], we tested four scenarios for each trait: (1) constant diversification (CR models), where speciation and extinction parameters are fixed to be the same across all states. (2) Variable diversification rates across the observed traits, without hidden traits. (3) Variable diversification rates across the observed traits, with hidden traits. (4) Variable diversification, but only across hidden states. For the SecSSE analysis, the number of parameters for hidden-state models was exceedingly large, and thus, only one hidden state (two rate categories) could be tested. Starting values for speciation and extinction were optimized with the bd_ML function from the R package DDD v5.0105 [76]. We ranked models according to their performance based on AIC and AICw to compare the fit of the four diversification scenarios. For the best-performing models, we estimated net diversification rates (speciation minus extinction) for each observed state to facilitate comparison. State-specific sampling fractions (species sampled in phylogeny/species sampled for state) were used to account for sampling biases. We applied SecSSE analysis on the 100 trees generated by treePL to account for uncertainty.

3. Results

(a) Phylogenetic relationship

Our AHE sequencing generated 150 high-quality loci for 124 toad species (electronic supplementary material, figure S1), with a missing data rate of 0.7%. These loci had a concatenated length of 184 074 bp, with an average locus length of 1227 bp. The combined dataset, including additional species, spanned 195 795 bp across 456 species.

Both the RAxML analysis of the AHE dataset (electronic supplementary material, figure S2) and ASTRAL analysis (electronic supplementary material, figure S3) produced similar topologies (normalized Robinson–Foulds distance = 0.04), with only minor conflicts in the placement of a few genera, such as *Phrynoidis asper*. Thirteen well-supported clades were identified from the AHE dataset alone (electronic supplementary material, figure S2). Our results strongly support the Central American lineage *Incilius* as the sister group to the North American *Anaxyrus* lineage, with both forming a sister clade to the South American

Rhinella (Clade 7 in electronic supplementary material, figure S2). Furthermore, the African genus *Sclerophrys* was shown to be non-monophyletic only due to '*S. dodsoni*' and a similar northeast African sample being sister to (and thus members of) *Vandijkophrynus*, with strong support (clade 13 in electronic supplementary material, figure S2). The African genera *Capensibufo*, *Poyntonophrynus*, and *Mertensophryne* form a monophyletic clade (Clade 12 in electronic supplementary material, figure S2). The generic monophyly of *Bufotes* from Asia was confirmed with high support (Clades 12 and 10 in electronic supplementary material, figure S2).

The ML tree constructed from the combined dataset showed a slight decrease in support (electronic supplementary material, figure S4), though the overall topology remained consistent with the AHE dataset. All 13 well-supported clades were retained, with identical positions and relationships (electronic supplementary material, figure S2). As anticipated, some inconsistencies around taxonomic identification arose in the combined dataset, due to misidentifications inherent with the use of GenBank data; however, this does not affect our overall conclusions.

(b) Biogeographic history and diversification dynamics

Our time-calibrated phylogeny and biogeographical analysis provided a clear timeframe for the global expansion of true toads. Ancestral area reconstruction, based on best-fit model (DEC +j; electronic supplementary material, table S7), indicated a South American origin for Bufonidae, with dispersal out of South America beginning in the Oligocene (figure 2*a*,*b*; Node 1 in electronic supplementary material, figure S5). The analysis further revealed that ancestral toads dispersed from South America into Africa around 29.0 Ma (figure 2*a*,*b*; Node 7 in electronic supplementary material, figure S5), which subsequently led to the diversification of African and Eurasian clades. In the New World, colonization of North America occurred via two distinct pathways. The first involved direct dispersal to North America around 31.3 Ma (figure 2*a*,*b*; Node 6 in electronic supplementary material, figure S5, leading to Clade 6 or *Peltophryne*), while the second pathway involved stepwise dispersal through Central America between 27.9 and 16.1 Ma. Throughout all these colonization processes, our analyses detected no secondary invasion events back into South America (figure 2*b*; electronic supplementary material, figure S5). Dispersal out of South America involved both direct expansion to Africa (rejecting M1) and movement towards Central and North America (rejecting M2). Within the M3 scenarios, there was no evidence of dispersal between North America and Europe (rejecting M3 and M3b) or between North America and Asia (rejecting M3a). Taken together, our results support the M3c scenario, indicating not only a Trans-Atlantic oceanic dispersal from South America to Africa and then the rest of the Old World, but also a separate dispersal from South America to North America, with no subsequent exchange between North America and the Old World (either Europe or Asia).

The BAMM analyses depicted a near hump-shaped increase in net diversification rates (figure 2*c*; electronic supplementary material, figure S6). Initially, diversification rates remained relatively flat until approximately 30 Ma, followed by a rapid increase until around 22 Ma (figure 2*c*). Thereafter, diversification rates gradually decreased over time, continuing to decline towards the present day (figure 2*c*).

In the fossil-based PyRate analyses, speciation rate and extinction most of the time remain constant, only recent extinction rate shifts are detected since 1.9 Ma, leading to a similar decreasing trend of net diversification rates (electronic supplementary material, figure S7).

(c) Trait diversification dynamics

Ancestral state reconstructions revealed clear patterns for most traits, except for adult habitat types (figure 3). The most recent common ancestor of extant toads was inferred to have been small in size (<50 mm; figure 3*a*), with other size classes emerging during the Oligocene (approx. 32 Ma). Larger body sizes appeared progressively later and were primarily restricted to the Northern Hemisphere (electronic supplementary material, figure S8), with the largest size class (>150 mm) being the most recent and involving relatively few species. The ancestral toad is also inferred to have lacked parotoid glands (figure 3*b*) and inguinal fat bodies (figure 3*e*). The acquisition of parotoid glands and inguinal fat bodies began around the Oligocene (approx. 32 Ma) and subsequently became widespread across most regions (electronic supplementary material, figures S9 and S10). The reconstruction of adult habitat types remains ambiguous at the root and across most internal nodes (figure 3*c*; electronic supplementary material, figure S11). The ancestral developmental mode was exotrophic, with larvae deriving energy from ingested food as free-swimming individuals (figure 3*d*; electronic supplementary material, figure S12). This developmental mode has been retained by most extant toads, except for a few specific lineages, such as *Nectophrynoides*, *Oreophrynella* and *Pelophryne*, which evolved endotrophic larval feeding.

The best-fitting models from SecSSE revealed a complex relationship between species diversification and trait evolution (figure 4; electronic supplementary material, table S8). For body size, the best-fitting model was a constant-diversification model (AICw = 1; figure 4*a*; electronic supplementary material, table S8), indicating that neither the observed states nor hidden states influenced diversification rates. In contrast, for the presence of parotoid glands, the best-fitting model supported contributions from both the observed state and a hidden state (AICw = 0.89; electronic supplementary material, table S8). The SecSSE model estimated significantly higher diversification rates (averaged across observed and hidden states) for species with parotoid glands (0.05–0.1 lineages Myr^{-1}) compared to those without (0.03–0.07 lineages Myr^{-1}, $p < 0.001$; figure 4*b*; electronic supplementary material, table S8). Similarly, for adult habitat types, the model also supported contributions from both observed and hidden states (AICw = 1; electronic supplementary material, table S8). Species with water-independent adult habitats exhibited significantly higher diversification rates (0.05–0.07 lineages Myr^{-1}) than those with water-dependent habitats

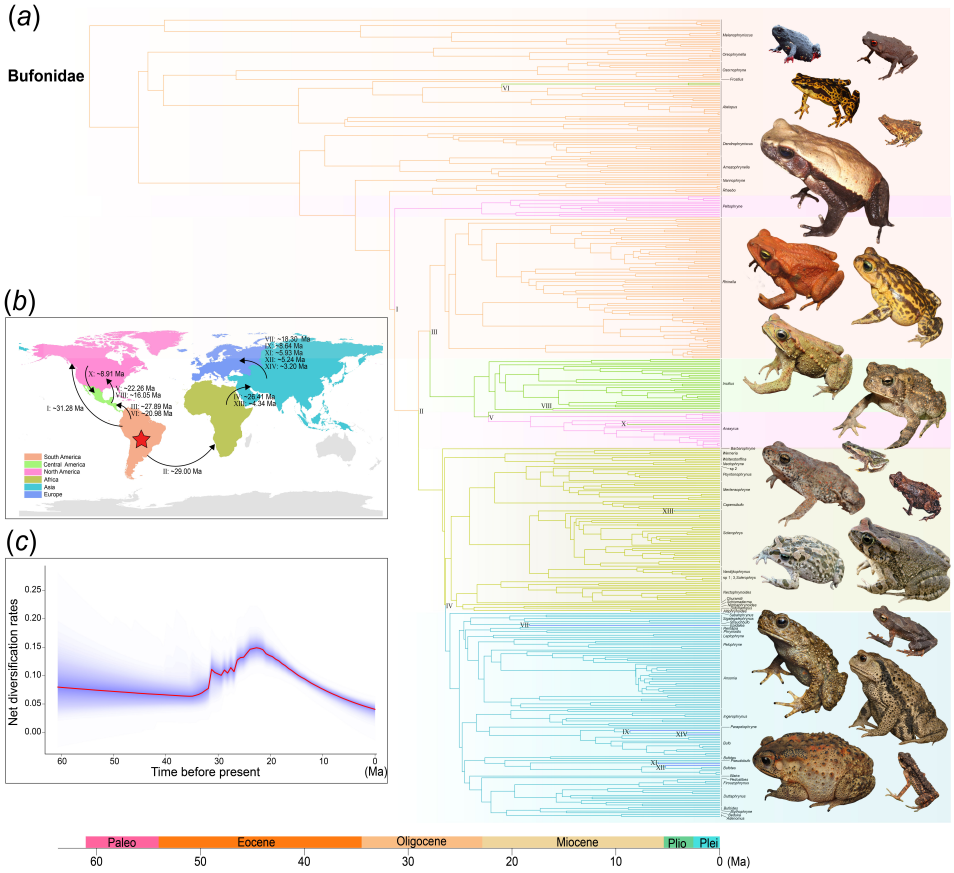

Figure 2. Ancestral area reconstruction and temporal dynamics of species diversification in modern toads. (*a*) Results of ancestral area reconstruction, with each colour representing a different region: orange for South America, light green for Central America, pink for North America, dark green for Africa, blue for Asia and purple for Europe. Tree markers indicate inferred cross-continental dispersal events, corresponding to the sequence illustrated in panel (*b*). Species photos courtesy of Ariel Rodriguez, Brian Freiermuth, Jörn Köhler, Mauro Teixeira Jr, Paul Szekely, Pedro L. V. Peloso, Robson W. Ávila, Sean M. Rovito, Stuart V. Nielsen, Thomas Eimermacher, Todd W. Pierson, Xiaolong Liu and Xianqi Li. (*b*) Schematic representation of cross-continental dispersal events, with timing estimated based on the oldest colonization events. The red star indicates the origin of Bufonidae. (*c*) Diversification rate estimates from BAMM analysis.

(0.03–0.06 lineages Myr^{-1}, $p < 0.001$; figure 4*c*; electronic supplementary material, table S8). For developmental modes, the model supported an effect of hidden states alone on diversification (AICw = 0.89; figure 4*d*; electronic supplementary material, table S8). In the case of inguinal fat bodies, both observed and hidden states were again supported as contributing factors (AICw = 1), with species possessing inguinal fat bodies showing significantly higher diversification rates (0.05–0.06 lineages Myr^{-1}) than those lacking them (0.02–0.03 lineages Myr^{-1}, $p < 0.001$; figure 4*e*; electronic supplementary material, table S8).

4. Discussion

Modern toads represent one of the few amphibian radiations to achieve a near-global distribution, yet their biogeographic history has long been debated. Our study resolves several persistent controversies by reconstructing a well-supported phylogeny and conducting formal biogeographic analysis. Together, these results reveal that modern toads most likely originated in South America and colonized the Old World via a Trans-Atlantic oceanic route, rather than through northern land bridges such as Beringia or the North Atlantic corridor.

Divergence time estimates place the origin of modern toads at 60.7 Ma (figure 2), well after the final breakup of the Gondwanan supercontinents, by which time South America and Africa had already separated [77,78]. This timeline renders a Gondwanan origin, as proposed by Maxson [37], less unlikely. Ancestral area reconstruction clearly supports an 'Out of South America' pattern (figure 2), consistent with previous studies such as Pramuk *et al.* [34], Van Bocxlaer *et al.* [24] and Pyron [35]. Notably, Pramuk *et al.* [34] inferred a South American origin from phylogenetic inference alone, without formal biogeographic modelling, while Van Bocxlaer *et al.* [24] and Pyron [35] integrated both divergence dating and quantitative biogeographic methods to support the same conclusion. Regarding the dispersal route to the Old World, Pramuk *et al.* [34] considered Beringia and the North Atlantic land bridges and tentatively favoured Beringia; however, their analysis was limited by sparse sampling and unresolved phylogenetic relationships, and lacked explicit biogeographic inference. In contrast, our results provide no evidence for post-origin dispersal between North America and Eurasia (figure 2*b*). Instead, we identified a strongly supported phylogenetic connection between South American and African lineages (figure 2*a*,*b*), suggesting a Trans-Atlantic oceanic dispersal event.

The trans-oceanic dispersal route from South America to Africa identified in our study includes two possibilities within the Cenozoic geological framework: (i) a single, long-distance overwater dispersal (rafting) or (ii) a stepwise migration through temperate–subtropical Antarctica. Traditionally, overwater dispersal by amphibians was considered improbable due to their

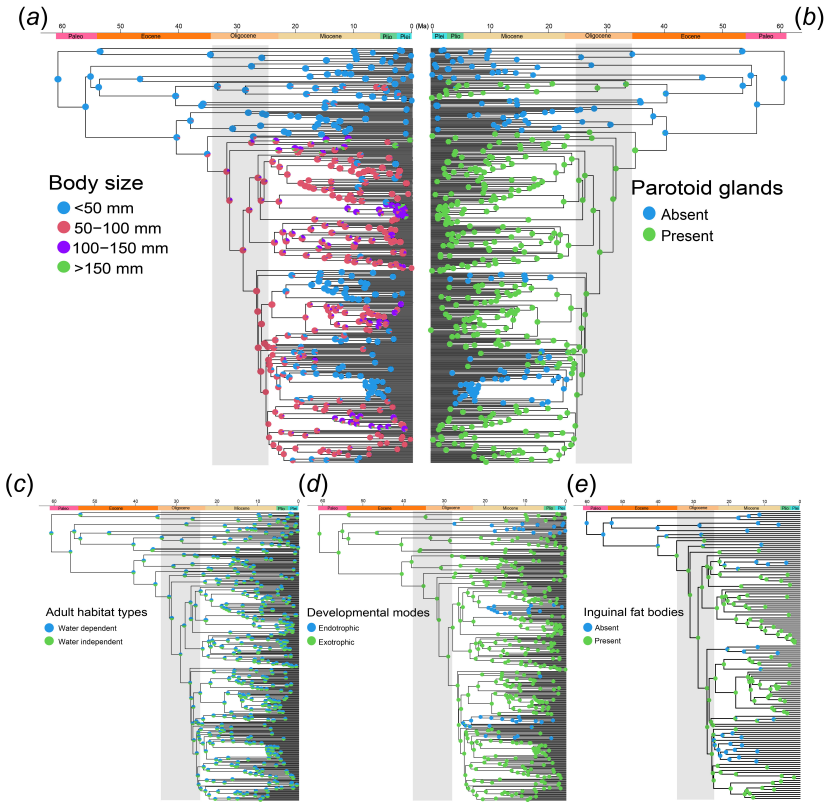

Figure 3. Ancestral state reconstruction of traits in modern toads. (*a*) Body size, categorized into four states: <50 mm, 50–100 mm, 100–150 mm and >150 mm. Results indicate that <50 mm was the ancestral state in modern toads. (*b*) Parotoid glands presence/absence. The absence of parotoid glands was inferred as the ancestral condition. (*c*) Adult habitat types, categorized as either water-dependent or water-independent. The ancestral state was ambiguous for this trait. (*d*) Developmental modes, categorized as endotrophic or exotrophic. The exotrophic mode was inferred to be the ancestral state. Grey shading denotes the time window corresponding to the initial dispersal out of South America. (*e*) Inguinal fat bodies presence/absence. The absence of inguinal fat bodies represents the ancestral condition.

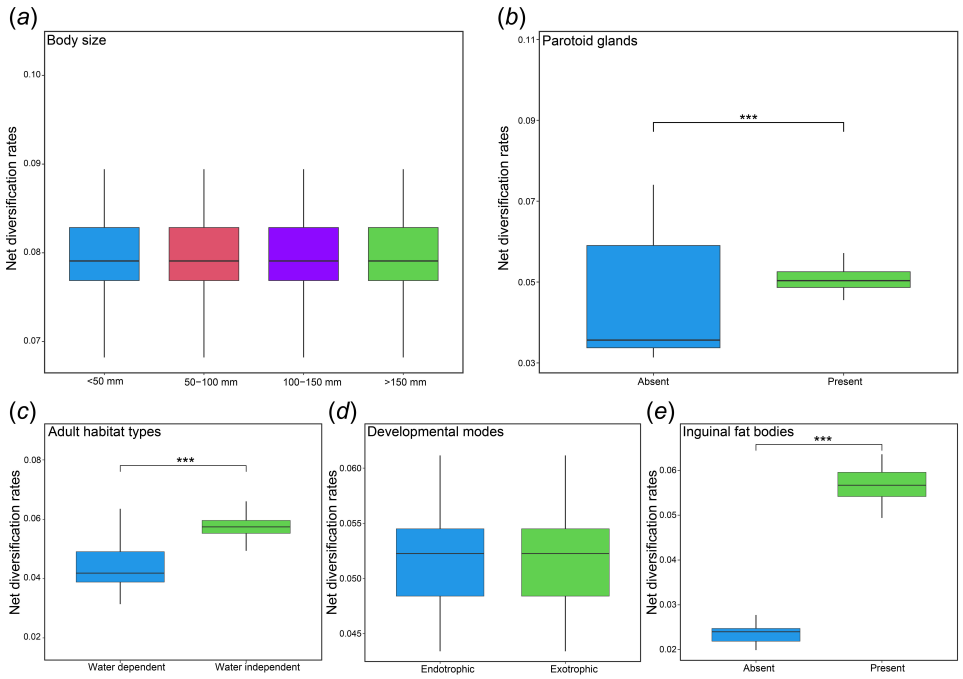

Figure 4. Diversification rates for each trait state are estimated under the best-fitting SecSSE model across 100 iterations. Panels show results for (*a*) body size, (*b*) parotoid glands, (*c*) adult habitat type, (*d*) developmental mode and (*e*) inguinal fat bodies.

salt intolerance [79,80]. However, accumulating evidence, including molecular clock data, island endemism patterns and direct observations of storm-driven rafting events covering thousands of kilometres, supports the feasibility of long-distance dispersal across oceans [81–84]. Alternatively, a stepwise dispersal via Antarctica is also feasible, given the continent's temperate to subtropical climate during the Late Cretaceous and early Cenozoic (100–50 Ma), as indicated by fossil plants, sediments and

geochemical proxies [85]. Intermittent land connections may have persisted until at least 31 Ma [86], which aligns with our divergence-time estimates for the initial expansion of modern toads from South America.

Although the role of Antarctica in amphibian dispersal has been rarely discussed (but see Goin & Goin [87]), the discovery of calyptocephalellid frog fossils in Antarctica [88] provides compelling evidence, and biotic exchanges between Antarctica and Africa have been suggested for other groups as well [89–91]. Similar biogeographic patterns have been proposed for pelodryadine hylids in Australasia, with both overwater dispersal from South America and stepwise dispersal via Antarctica suggested as plausible scenarios [17,35]. Determining which, if either, of these pathways predominated remains an open question; resolving it will require denser fossil sampling, more comprehensive molecular datasets and higher-resolution palaeogeographic models. In summary, our results highlight the need to seriously consider both oceanic and Antarctic corridors in reconstructing amphibian biogeography and demonstrate that, under favourable climatic and geological conditions, even physiologically constrained groups like amphibians can overcome formidable geographic barriers.

Our analysis reveals a marked acceleration in species diversification rates shortly after the rapid expansion of modern toads out of South America, echoing patterns observed by Van Bocxlaer *et al.* [24], although their study did not explicitly address geological drivers of diversification. This pulse coincides with the Eocene—Oligocene transition—a global extinction event that likely opened ecological niches for colonization and diversification [92–95]. Following their colonization in Africa, modern toads dispersed into Asia via the Middle East and colonized Europe through five independent events after the closure of the Tethys Ocean (figure 2*b*). The Terminal Tethyan Event (18–12 Ma) possibly facilitated the dispersal between Africa and Eurasia through plate connection by tectonic movement and convergence [96–98]. In the New World, modern toads dispersed from South to North America via both direct and stepwise routes well before the Isthmus of Panama closed, paralleling patterns observed in genus *Rana* (Ranidae, Amphibia) [99–101]. Although fossil-based estimates suggest a recent extinction during the glacial period (electronic supplementary material, figure S7), these appear to have had a limited impact on overall toad diversity or distribution. Together, these patterns highlight the group's exceptional capacity to overcome geographic barriers, rapidly colonize new environments and establish populations across broad geographic regions.

The acceleration in modern toads' diversification and subsequent rapid expansion also matches with the evolution of key innovation traits, such as the emergence of parotoid glands; however, other traits did not show such an association. The evolution of parotoid glands, a novel pair of dorsolateral organs on the toad's head that secrete toxins which are highly repellent to many predators, has been recognized as another major factor contributing to the successful modern invasion of cane toads into Australia [102]. This evolutionary innovation emerging immediately after the dispersal from South America, underwent rapid phenotypic evolution in lineages that left the continent, while also contributing to species diversification (figure 4). The emergence of this organ enabled toads with this trait to achieve greater global dominance in species composition compared to those characterized by larger body size (electronic supplementary material, figure S10). A similar diversification pattern may exist for inguinal fat bodies—another trait hypothesized to facilitate physiological adaptation in harsh habitats—but because current sampling for this character is relatively limited, we can only make preliminary conclusions at this time.

Body size is often considered a key factor in the success of the cane toad (*Rhinella marina*), a species that originated in Central and South America and has since invaded many geographic areas through direct human introductions, rapidly spreading across Australia on a continental scale [103]. Increased body size allows toads to effectively respond to environmental changes across diverse local conditions, with aridity being an important barrier to be faced [104]. It may also facilitate range expansion by reducing water loss due to optimized surface-to-volume ratios [105–107]. In our study, the emergence of larger body size closely coincided with the timing of the Old-World colonization (figure 3*a*). However, body size showed no significant association with species diversification (figure 4), which may explain why large-bodied species are predominantly restricted to the Northern Hemisphere (electronic supplementary material, figure S8). Traits such as adult habitat types and developmental modes, while crucial for toad survival in harsh environments, do not appear to be associated with high diversification rates (figure 4) and global expansion (figure 3*c*,*d*). This lack of correlation may reflect that, while generalist physiological adaptations of amphibians can enhance survival in marginal environments, they may lack the functional specificity or ecological impact necessary to drive rapid radiations or facilitate long-distance dispersal—unlike more specialized traits for modern toads such as the parotoid glands and inguinal fat bodies (figure 4).

In conclusion, our study suggests that the global radiation of toads is closely linked to both geological history and trait innovation. Geological changes, particularly during the Oligocene and Miocene, facilitated the colonization of the Old World, while the emergence of innovative traits, especially the parotoid glands, enabled toads to flourish in new environments (with new predators), diversify rapidly and occupy various ecological niches. This research provides a compelling example of integrating historical biogeography and trait evolution to elucidate the processes underlying global diversity patterns. Further studies are needed to deepen our understanding of these dynamics.

Ethics. All sample collections were performed according to the ethical guidelines approved by the Institutional Animal Care and Use Committee (IACUC) of Southwest University (approval no. LAC2023-2-0091).

Data accessibility. The data and codes are available Zenodo [108] and from the Dryad Digital Repository [109].

Supplementary material is available online [110].

Declaration of AI use. We have not used AI-assisted technologies in creating this article.

Authors' contributions. D.W.: data curation, investigation, methodology, visualization, writing—original draft; E.P.: conceptualization, resources, writing—review and editing; C.J.R.: resources, supervision, writing—review and editing; Z.W.: supervision, writing—review and editing; W.Z.: conceptualization, writing—review and editing; J.C.: conceptualization, writing—review and editing; C.S.: funding acquisition, resources, supervision, writing—review and editing; P.S.: conceptualization, resources, writing—review and editing; M.R.P.: conceptualization, resources, writing—review and editing; W.X.: conceptualization, funding acquisition, methodology, supervision, writing—original draft, writing—review and editing; Z.Y.: conceptualization, funding acquisition, project administration, resources, writing—review and editing.

All authors gave final approval for publication and agreed to be held accountable for the work performed therein.

Conflict of interest declaration. We declare we have no competing interests.

Funding. This work was funded by the National Natural Science Foundation of China (NSFC32170478, NSFC32370478, NSFC32300383, NSFC32470458, NSFC32170445) to Z.Y.Y., W.X., J.M.C. and W.W.Z., Fundamental Research Funds for the Central Universities (SWU-KR22014) to Z.Y.Y., Youth Top Talent Program of Chongqing (CQYC20220510893) to Z.Y.Y., Conservation and Genetic Germplasm Creation of Aquatic Resources in the Upper Yangtze River (2010423005) to Z.Y.Y., Special Fund for Youth Team of Southwest University (SWU-XJPY202302) to Z.Y.Y., Science and Technology Projects of Xizang Autonomous Region, China (program no. XZ202402ZD0005) to Z.Y.Y., Thailand Science Research and Innovation Fund and the University of Phayao (Unit of Excellence 2026 on Aquatic animals biodiversity assessment (phase II)), the Institutional Ethical Committee of Animal Experimentation of the University of Phayao (UP-AE59-01-04-0022); and the National Science Foundation (USA) BIO-DEB 1021247 to E.P. and C.J.R.

Acknowledgements. We thank the following institutions and individuals for providing access to critical tissue samples: American Museum of Natural History (David Kizirian); California Academy of Sciences (Lauren A. Scheinberg); Field Museum of Natural History (Sara Ruane, Josh Mata, Terry A. Lott, Alan Resetar); Royal Ontario Museum (Robert W. Murphy, Amy Lathrop); Museum of Comparative Zoology, Harvard University (Jim Hanken, Joel Martinez, Breda M. Zimkus, Emily Blank); Museum of Vertebrate Zoology, University of California, Berkeley (Jimmy A. McGuire, Carol L. Spencer); University of Florida (David C. Blackburn); South African Institute for Aquatic Biology (Roger Bills). For additional samples, we thank Aaron Bauer, Raj Patel, Simon Loader, and Eli Greenbaum; College of Life Sciences, Anhui Normal University (Song Huang); The Germplasm Bank of Wild Species in Southwest China (Jing Che, Jieqiong Jin). We thank Jing Che, Chenhong Li, Wei Gao, Yunhe Wu, Kai Wang, Song Huang, Pingfan Wei and Xiaolong Liu for their help in sample collection and analysis. We are also grateful to the three anonymous reviewers for their constructive comments and suggestions, which significantly improved the quality of this manuscript.

References

1. MacArthur RH, Wilson EO. 1967 *The theory of island biogeography*. Princeton, NJ: Princeton University Press.
2. Lomolino MV, Riddle BR, Whittaker RJ. 2017 *Biogeography: biological diversity across space and time*. Sunderland, MA: Sinauer Associates Inc. (doi:10.1093/hesc/9781605354729.001.0001)
3. Smith AC, Smith DG, Funnell BM. 1994 *Atlas of Mesozoic and Cenozoic coastlines*. New York, NY: Cambridge University Press.
4. Upchurch P. 2008 Gondwanan break-up: legacies of a lost world? *Trends Ecol. Evol*. **23**, 229–236. (doi:10.1016/j.tree.2007.11.006)
5. Wallace AR. 1863 On the physical geography of the Malay Archipelago. *J. R. Geogr. Soc. Lond*. **7**, 206–213. (doi:10.2307/1799061)
6. Lohman DJ, de Bruyn M, Page T, von Rintelen K, Hall R, Ng PKL, Shih HT, Carvalho GR, von Rintelen T. 2011 Biogeography of the Indo-Australian archipelago. *Annu. Rev. Ecol. Evol. Syst*. **42**, 205–226. (doi:10.1146/annurev-ecolsys-102710-145001)
7. Simpson GG. 1980 *Splendid isolation: the curious history of South American mammals*. New Haven, CT: Yale University Press.
8. Jaramillo CA. 2018 Evolution of the Isthmus of Panama: biological, paleoceanographic and paleoclimatological implications. In *Mountains, climate and biodiversity* (eds Hoorn C, Perrigo A, Antonelli A), pp. 323–338. Oxford, UK: Wiley Blackwell.
9. Stigall AL. 2019 The invasion hierarchy: ecological and evolutionary consequences of invasions in the fossil record. *Annu. Rev. Ecol. Evol. Syst*. **50**, 355–380. (doi:10.1146/annurev-ecolsys-110617-062638)
10. Rosenzweig ML. 1995 *Species diversity in space and time*. New York, NY: Cambridge University Press.
11. Wiens JJ, Donoghue MJ. 2004 Historical biogeography, ecology and species richness. *Trends Ecol. Evol*. **19**, 639–644. (doi:10.1016/j.tree.2004.09.011)
12. Fine PVA. 2015 Ecological and evolutionary drivers of geographic variation in species diversity. *Annu. Rev. Ecol. Evol. Syst*. **46**, 369–392. (doi:10.1146/annurev-ecolsys-112414-054102)
13. Sanmartín I, EnghoffH, RonquistF. 2001 Patterns of animal dispersal, vicariance and diversification in the holarctic. *Biol. J. Linn. Soc*. **73**, 345–390. (doi:10.1006/bijl.2001.0542)
14. Yoder AD, Nowak MD. 2006 Has vicariance or dispersal been the predominant biogeographic force in Madagascar? Only time will tell. *Annu. Rev. Ecol. Evol. Syst*. **37**, 405–431. (doi:10.1146/annurev.ecolsys.37.091305.110239)
15. Sanmartín I, Ronquist F. 2004 Southern Hemisphere biogeography inferred by event-based models: plant versus animal patterns. *Syst. Biol*. **53**, 216–243. (doi:10.1080/10635150490423430)
16. Wright TF *et al*. 2008 A multilocus molecular phylogeny of the parrots (Psittaciformes): support for a Gondwanan origin during the Cretaceous. *Mol. Biol. Evol*. **25**, 2141–2156. (doi:10.1093/molbev/msn160)
17. Feng YJ, Blackburn DC, Liang D, Hillis DM, Wake DB, Cannatella DC, Zhang P. 2017 Phylogenomics reveals rapid, simultaneous diversification of three major clades of Gondwanan frogs at the Cretaceous–Paleogene boundary. *Proc. Natl Acad. Sci. USA* **114**, 5864–5870. (doi:10.1073/pnas.1704632114)
18. Yuan ZY *et al*. 2018 Natatanuran frogs used the Indian plate to step-stone disperse and radiate across the Indian Ocean. *Nat. Sci. Rev*. **6**, 10–14. (doi:10.1093/nsr/nwy092)
19. Toon A, Pérez-Losada M, Schweitzer CE, Feldmann RM, Carlson M, Crandall KA. 2010 Gondwanan radiation of the Southern Hemisphere crayfishes (Decapoda: Parastacidae): evidence from fossils and molecules. *J. Biogeogr*. **37**, 2275–2290. (doi:10.1111/j.1365-2699.2010.02374.x)
20. Wiens JJ. 2023 Trait-based species richness: ecology and macroevolution. *Biol. Rev*. **98**, 1365–1387. (doi:10.1111/brv.12957)
21. Yoder JB *et al*. 2010 Ecological opportunity and the origin of adaptive radiations. *J. Evol. Biol*. **23**, 1581–1596. (doi:10.1111/j.1420-9101.2010.02029.x)
22. Miller AH, Stroud JT, Losos JB. 2023 The ecology and evolution of key innovations. *Trends Ecol. Evol*. **38**, 122–131. (doi:10.1016/j.tree.2022.09.005)
23. Fei L, Hu SQ, Ye CY, Huang YZ. 2009 *Fauna Sinica, Amphibia, vol. 2, Anura*. Beijing, Peoples's Republic of China: Beijing Science Press.
24. Van Bocxlaer I, Loader SP, Roelants K, Biju SD, Menegon M, Bossuyt F. 2010 Gradual adaptation toward a range-expansion phenotype initiated the global radiation of toads. *Science* **327**, 679–682. (doi:10.1126/science.1181707)
25. AmphibiaChina. 2023 *The database of Chinese amphibians*. Kunming Institute of Zoology. See http://www.amphibiachina.org/ (accessed 1 March 2023).
26. Richard S. 2010 The ecological impact of invasive cane toads (*Bufo marinus*) in Australia. *Q. Rev. Biol*. **4**, 1–84. (doi:10.1086/655116)
27. Marshall BM. 2018 *Investigating the potential susceptibility of selected Malagasy species to the toxins produced by Duttaphrynus melanostictus (Asian common toad)*. Bangor, UK: Bangor University.
28. Baxter-Gilbert J, Florens FBV, Baider C, Perianen YD, Citta DS, Appadoo C, Measey J. 2021 Toad-kill: prey diversity and preference of invasive guttural toads (*Sclerophrys gutturalis*) in Mauritius. *Afr. J. Ecol*. **59**, 168–177. (doi:10.1111/aje.12814)
29. AmphibiaWeb. 2023 AmphibiaWeb. Berkeley, CA, USA: University of California. See https://amphibiaweb.org/ (accessed 1 March 2023).

30. Liedtke HC *et al*. 2016 No ecological opportunity signal on a continental scale? Diversification and life-history evolution of African true toads (Anura: Bufonidae). *Evolution* **70**, 1717–1733. (doi:10.1111/evo.12985)
31. Jin L, Yu JP, Yang ZJ, Merilä J, Liao WB. 2018 Modulation of gene expression in liver of hibernating Asiatic Toads (*Bufo gargarizans*). *Int. J. Mol. Sci*. **19**, 2363. (doi:10.3390/ijms19082363)
32. Cesare P, Bonfigli A, Miranda M, Poma AM, Colafarina S, Zarivi O. 2019 Transcriptional analysis of tyrosinase gene expression during *Bufo bufo* development. *Saudi J. Biol. Sci*. **26**, 8–19. (doi:10.1016/j.sjbs.2016.10.018)
33. Blair WF. 1972 Summary. In *Evolution in the genus Bufo* (ed. WF Blair), pp. 329–343. Austin, TX, USA: University Texas Press.
34. Pramuk JB, Robertson T, Sites JW Jr, Noonan BP. 2008 Around the world in 10 million years: biogeography of the nearly cosmopolitan true toads (Anura: Bufonidae). *Glob. Ecol. Biogeogr*. **17**, 72–83. (doi:10.1111/j.1466-8238.2007.00348.x)
35. Pyron RA. 2014 Biogeographic analysis reveals ancient continental vicariance and recent oceanic dispersal in Amphibians. *Syst. Biol*. **63**, 779–797. (doi:10.1093/sysbio/syu042)
36. Tihen JA. 1962 Osteological observations on New World *Bufo*. *Am. Midl. Nat*. **67**, 157–183. (doi:10.2307/2422826)
37. Maxson LR. 1984 Molecular probes of phylogeny and biogeography in toads of the widespread genus *Bufo*. *Mol. Biol. Evol*. **1**, 345–356. (doi:10.1093/oxfordjournals.molbev.a040323)
38. Donoghue MJ, Smith SA. 2004 Patterns in the assembly of temperate forests around the Northern Hemisphere. *Proc. R. Soc. B* **359**, 1633–1644. (doi:10.1098/rstb.2004.1538)
39. Lemmon AR, Emme SA, Lemmon EM. 2012 Anchored hybrid enrichment for massively high-throughput phylogenomics. *Syst. Biol*. **61**, 727–744. (doi:10.1093/sysbio/sys049)
40. Hime PM *et al*. 2021 Phylogenomics reveals ancient gene tree discordance in the amphibian tree of life. *Syst. Biol*. **70**, 49–66. (doi:10.1093/sysbio/syaa034)
41. Pyron RA, Wiens JJ. 2011 A large-scale phylogeny of Amphibia including over 2800 species, and a revised classification of extant frogs, salamanders, and caecilians. *Mol. Phylogenet. Evol*. **61**, 543–583. (doi:10.1016/j.ympev.2011.06.012)
42. Mandel JR, Dikow RB, Funk VA, Masalia RR, Staton SE, Kozik A, Michelmore RW, Rieseberg LH, Burke JM. 2014 A target enrichment method for gathering phylogenetic information from hundreds of loci: an example from the compositae. *Appl. Plant Sci*. **2**, 1300085. (doi:10.3732/apps.1300085)
43. Bolger AM, Lohse M, Usadel B. 2014 Trimmomatic: a flexible trimmer for Illumina sequence data. *Bioinformatics* **30**, 2114–2120. (doi:10.1093/bioinformatics/btu170)
44. Johnson MG, Gardner EM, Liu Y, Medina R, Goffinet B, Shaw AJ, Zerega NJC, Wickett NJ. 2016 HybPiper: extracting coding sequence and introns for phylogenetics from high-throughput sequencing reads using target enrichment. *Appl. Plant Sci*. **4**, 1600016. (doi:10.3732/apps.1600016)
45. Li H, Durbin R. 2009 Fast and accurate short read alignment with Burrows–Wheeler transform. *Bioinformatics* **25**, 1754–1760. (doi:10.1093/bioinformatics/btp324)
46. Bankevich A *et al*. 2012 SPAdes: a new genome assembly algorithm and its applications to single-cell sequencing. *J. Comput. Biol*. **19**, 455–477. (doi:10.1089/cmb.2012.0021)
47. Katoh K, Standley DM. 2013 MAFFT multiple sequence alignment software version 7: improvements in performance and usability. *Mol. Biol. Evol*. **30**, 772–780. (doi:10.1093/molbev/mst010)
48. Capella-Gutiérrez S, Silla-Martínez JM, Gabaldón T. 2009 trimAl: a tool for automated alignment trimming in large-scale phylogenetic analyses. *Bioinformatics* **25**, 1972–1973. (doi:10.1093/bioinformatics/btp348)
49. Jetz W, Pyron RA. 2018 The interplay of past diversification and evolutionary isolation with present imperilment across the amphibian tree of life. *Nat. Ecol. Evol*. **2**, 850–858. (doi:10.1038/s41559-018-0515-5)
50. Portik DM, Streicher JW, Wiens JJ. 2023 Frog phylogeny: a time-calibrated, species-level tree based on hundreds of loci and 5,242 species. *Mol. Phylogenet. Evol*. **188**, 107907. (doi:10.1016/j.ympev.2023.107907)
51. Stamatakis A. 2014 RAxML version 8: a tool for phylogenetic analysis and post-analysis of large phylogenies. *Bioinformatics* **30**, 1312–1313. (doi:10.1093/bioinformatics/btu033)
52. Mirarab S, Reaz R, Bayzid M, Zimmermann T, Swenson MS, Warnowl T. 2014 ASTRAL: genome-scale coalescent-based species tree estimation. *Bioinformatics* **30**, i541–i548. (doi:10.1093/bioinformatics/btu462)
53. Sayyari E, Mirarab S. 2016 Fast coalescent-based computation of local branch support from quartet frequencies. *Mol. Biol. Evol*. **33**, 1654–1668. (doi:10.1093/molbev/msw079)
54. Sanderson MJ. 2002 Estimating absolute rates of molecular evolution and divergence times: a penalized likelihood approach. *Mol. Biol. Evol*. **19**, 101–109. (doi:10.1093/oxfordjournals.molbev.a003974)
55. Smith SA, O'Meara BC. 2012 treePL: divergence time estimation using penalized likelihood for large phylogenies. *Bioinformatics* **28**, 2689–2690. (doi:10.1093/bioinformatics/bts492)
56. Báez AM, Nicoli L. 2004 Bufonid toads from the Late Oligocene beds of Salla Bolivia. *J. Vertebr. Paleontol*. **24**, 73–79. (doi:10.1671/1900-6)
57. Drummond AJ, Rambaut A. 2007 BEAST: Bayesian evolutionary analysis by sampling trees. *BMC Evol. Biol*. **7**, 1–8. (doi:10.1186/1471-2148-7-214)
58. Matzke NJ. 2013 BioGeoBEARS: biogeography with Bayesian and likelihood evolutionary analysis in R scripts. See http://cran.r-project.org/web/packages/BioGeoBEARS/.
59. Pauly GB, Hillis DM, Cannatella DC. 2004 The history of a Nearctic colonization: molecular phylogenetics and biogeography of the Nearctic toads (*Bufo*). *Evolution* **58**, 2517–2535. (doi:10.1111/j.0014-3820.2004.tb00881.x)
60. Pramuk JB. 2006 Phylogeny of South American *Bufo* (Anura: Bufonidae) inferred from combined evidence. *Zool. J. Linn. Soc*. **146**, 407–452. (doi:10.1111/j.1096-3642.2006.00255.x)
61. Ree RH, Smith SA. 2008 Maximum likelihood inference of geographic range evolution by dispersal, local extinction, and cladogenesis. *Syst. Biol*. **57**, 4–14. (doi:10.1080/10635150701883881)
62. Ronquist F. 1997 Dispersal-vicariance analysis: a new approach to the quantification of historical biogeography. *Syst. Biol*. **46**, 195–203. (doi:10.1093/sysbio/46.1.195)
63. Landis MJ, Matzke NJ, Moore BR, Huelsenbeck JP. 2013 Bayesian analysis of biogeography when the number of areas is large. *Syst. Biol*. **62**, 789–804. (doi:10.1093/sysbio/syt040)
64. Rabosky DL. 2014 Automatic detection of key innovations, rate shifts, and diversity-dependence on phylogenetic trees. *PLoS One* **92**, e89543. (doi:10.1371/journal.pone.0089543)
65. Rabosky DL, Grundler M, Anderson C, Title P, Shi JJ, Brown JW, Huang H, Larson JG. 2014 BAMMtools: an R package for the analysis of evolutionary dynamics on phylogenetic trees. *Methods Ecol. Evol*. **5**, 701–707. (doi:10.1111/2041-210x.12199)
66. Plummer M, Best N, Cowles K, Vines K. 2006 CODA: convergence diagnosis and output analysis for MCMC. *R News* **6**, 7–11. http://oro.open.ac.uk/22547/
67. Silvestro D, Salamin N, Antonelli A, Meyer X. 2019 Improved estimation of macroevolutionary rates from fossil data using a Bayesian framework. *Paleobiology* **45**, 546–570. (doi:10.1017/pab.2019.23)
68. Hauffe T, Cantalapiedra JL, Silvestro D. 2024 Trait-mediated speciation and human-driven extinctions in proboscideans revealed by unsupervised Bayesian neural networks. *Sci. Adv*. **10**, eadl2643. (doi:10.1126/sciadv.adl2643)
69. IUCN. 2023 The IUCN red list of threatened species. Version 2023. See https://www.iucnredlist.org/ (accessed 1 March 2023).
70. Bollback JP. 2006 SIMMAP: stochastic character mapping of discrete traits on phylogenies. *BMC Bioinform*. **7**, 88. (doi:10.1186/1471-2105-7-88)
71. Revell LJ. 2012 phytools: an R package for phylogenetic comparative biology (and other things). *Methods Ecol. Evol*. **3**, 217–223. (doi:10.1111/j.2041-210x.2011.00169.x)
72. Harmon LJ, Weir JT, Brock CD, Glor RE, Challenger W. 2007 GEIGER: investigating evolutionary radiations. *Bioinformatics* **24**, 129–131. (doi:10.1093/bioinformatics/btm538)

73. Burnham KP, Anderson DR. 2002 *Model selection and multimodel inference: a practical information-theoretic approach*, 2nd edn. New York, NY: Springer-Verlag.
74. Herrera-Alsina L, van Els P, Etienne RS. 2019 Detecting the dependence of diversification on multiple traits from phylogenetic trees and trait data. *Syst. Biol*. **68**, 317–328. (doi:10.1093/sysbio/syy057)
75. Liedtke HC, Wiens JJ, Gomez-Mestre I. 2022 The evolution of reproductive modes and life cycles in amphibians. *Nat. Commun*. **13**, 7039. (doi:10.1038/s41467-022-34474-4)
76. Etienne RS, Haegeman B. 2012 A conceptual and statistical framework for adaptive radiations with a key role for diversity dependence. *Am. Nat*. **180**, 75–89. (doi:10.1086/667574)
77. Pitman WC, Cande S, LaBrecque J, Pindell J, Goldblatt P. 1993 Fragmentation of Gondwana: the separation of Africa from South America. In *Biological relationships between africa and south america* (ed. P Goldblatt), pp. 3–14. New Haven, CT: Yale University Press. (doi:10.2307/j.ctt22726mc.5)
78. Maisey JG. 2000 Tectonics, the Santana Lagerstätten, and the Implications for late Gondwanan biogeography. In *Biological relationships between Africa and South America* (ed. P Goldblatt), pp. 435–454. New Haven, CT: Yale University Press. (doi:10.2307/j.ctt22726mc.18)
79. Van Bocxlaer I, Roelants K, Biju SD, Nagaraju J, Bossuyt F. 2006 Late Cretaceous vicariance in Gondwanan amphibians. *PLoS One* **1**, e74. (doi:10.1371/journal.pone.0000074)
80. Bossuyt F, Milinkovitch MC. 2001 Amphibians as indicators of early tertiary 'out-of-India' dispersal of vertebrates. *Science* **292**, 93–95. (doi:10.1126/science.1058875)
81. Vences M, Vieites DR, Glaw F, Brinkmann H, Kosuch J, Veith M, Meyer A. 2003 Multiple overseas dispersal in amphibians. *Proc. R. Soc. Lond. B* **270**, 2435–2442. (doi:10.1098/rspb.2003.2516)
82. de Queiroz A. 2005 The resurrection of oceanic dispersal in historical biogeography. *Trends Ecol. Evol*. **20**, 68–73. (doi:10.1016/j.tree.2004.11.006)
83. Measey GJ, Vences M, Drewes RC, Chiari Y, Melo M, Bourles B. 2007 Freshwater paths across the ocean: molecular phylogeny of the frog *Ptychadena* newtoni gives insights into amphibian colonization of oceanic islands. *J. Biogeogr*. **34**, 7–20. (doi:10.1111/j.1365-2699.2006.01589.x)
84. Bell RC, Drewes RC, Channing A, Gvoždík V, Kielgast J, Lötters S, Stuart BL, Zamudio KR. 2015 Overseas dispersal of *Hyperolius* reed frogs from Central Africa to the oceanic islands of São Tomé and Príncipe. *J. Biogeogr*. **42**, 65–75. (doi:10.1111/jbi.12412)
85. Francis JE, Poole I. 2002 Cretaceous and early tertiary climates of Antarctica: evidence from fossil wood. *Palaeogeogr. Palaeoclimatol. Palaeoecol*. **182**, 47–64. (doi:10.1016/s0031-0182(01)00452-7)
86. Blakely RC. 2008 Gondwana paleogeography from assembly to breakup–a 500 m.y. odyssey. *GSA Spec. Pap* **441**, 1–28. (doi:10.1130/2008.2441(01)
87. Goin CJ, Goin OB. 1972 Antarctica, isostacy, and the origin of frogs. *Q. J. Fla. Acad. Sci*. **35**, 113–129.
88. Mörs T, Reguero M, Vasilyan D. 2020 First fossil frog from Antarctica: implications for Eocene high latitude climate conditions and Gondwanan cosmopolitanism of Australobatrachia. *Sci. Rep*. **10**, 5051. (doi:10.1038/s41598-020-61973-5)
89. Crisp MD, Cook LG. 2013 How was the Australian flora assembled over the last 65 million years? A molecular phylogenetic perspective. *Annu. Rev. Ecol. Evol. Syst*. **44**, 303–324. (doi:10.1146/annurev-ecolsys-110512-135910)
90. Lawver LA, Gahagan LM. 2003 Evolution of Cenozoic seaways in the circum-Antarctic region. *Palaeogeogr. Palaeoclimatol. Palaeoecol*. **198**, 11–37. (doi:10.1016/s0031-0182(03)00392-4)
91. Ali JR, Krause DW. 2011 Late Cretaceous bioconnections between Indo-Madagascar and Antarctica: refutation of the gunnerus ridge causeway hypothesis. *J. Biogeogr*. **38**, 1855–1872. (doi:10.1111/j.1365-2699.2011.02546.x)
92. Berggren WA, Prothero DR. 1992 Eocene-Oligocene climatic and biotic evolution: an overview. In *Eocene-Oligocene climatic and biotic evolution* (eds DR Prothero, WA Berggren), pp. 1–28. Princeton, NJ: Princeton University Press. (doi:10.1515/9781400862924.1). See https://www.degruyter.com/document/doi/10.1515/9781400862924/html.
93. Retallack GJ, Orr WN, Prothero DR, Duncan RA, Kester PR, Ambers CP. 2004 Eocene-Oligocene extinction and paleoclimatic change near Eugene, Oregon. *Geol. Soc. Am. Bull*. **116**, 817–839. (doi:10.1130/B25281.1)
94. Prothero DR. 1994 The late eocene-oligocene extinctions. *Annu. Rev. Earth Planet. Sci*. **22**, 145–165. (doi:10.1146/annurev.ea.22.050194.001045)
95. Ivany LC, Patterson WP, Lohmann KC. 2000 Cooler winters as a possible cause of mass extinctions at the Eocene/Oligocene boundary. *Nature* **407**, 887–890. (doi:10.1038/35038044)
96. Adams CG, Gentry AW, Whybrow PJ. 1983 Dating the terminal Tethyan event. *Utrecht Micropal. Bull*. **30**, 273–298.
97. Steininger FF, Rögl F. 1984 Paleogeography and palinspastic reconstruction of the Neogene of the Mediterranean and Paratethys. *Geol. Soc. Lond. Spec. Publ*. **17**, 659–668. (doi:10.1144/gsl.sp.1984.017.01.52)
98. Gheerbrant E, Rage JC. 2006 Paleobiogeography of Africa: how distinct from Gondwana and Laurasia? *Palaeogeogr. Palaeoclimatol. Palaeoecol*. **241**, 224–246. (doi:10.1016/j.palaeo.2006.03.016)
99. Bacon CD, Silvestro D, Jaramillo C, Smith BT, Chakrabarty P, Antonelli A. 2015 Biological evidence supports an early and complex emergence of the Isthmus of Panama. *Proc. Natl Acad. Sci. USA* **112**, 6110–6115. (doi:10.1073/pnas.1423853112)
100. Montes C *et al*. 2015 Middle Miocene closure of the central American seaway. *Science* **348**, 226–229. (doi:10.1126/science.aaa2815)
101. Yuan ZY *et al*. 2016 Spatiotemporal diversification of the true frogs (genus *Rana*): a historical framework for a widely studied group of model organisms. *Syst. Biol*. **65**, 824–842. (doi:10.1093/sysbio/syw055)
102. Phillips BL, Shine R. 2005 The morphology, and hence impact, of an invasive species (the cane toad, *Bufo marinus*): changes with time since colonisation. *Anim. Conserv.* **8**, 407–413. (doi:10.1017/S1367943005002374)
103. Phillips BL, Brown GP, Greenlees M, Webb JK, Shine R. 2007 Rapid expansion of the cane toad (*Bufo marinus*) invasion front in tropical Australia. *Austral. Ecol*. **32**, 169–176. (doi:10.1111/j.1442-9993.2007.01664.x)
104. Hudson CM, Brown GP, Stuart K, Shine R. 2018 Sexual and geographical divergence in head widths of invasive cane toads, *Rhinella marina* (Anura: Bufonidae), is driven by both rapid evolution and plasticity. *Biol. J. Linn. Soc*. **124**, 188–199. (doi:10.1093/biolinnean/bly040)
105. Schmid WD. 1965 Some aspects of the water economies of nine species of amphibians. *Ecology* **46**, 261–269. (doi:10.2307/1936329)
106. Bentley PJ. 1966 Adaptations of Amphibia to arid environments: novel physiological mechanisms not seen in fish aid frogs and toads to conserve water and live in deserts. *Science* **152**, 619–623. (doi:10.1126/science.152.3722.619)
107. Szarski H. 1972 *Evolution in the Genus Bufo*, (ed. WF Blair), pp. 71–82. Austin, TX: University Texas Press.
108. Wu D. 2025 Earth history and trait innovation drive the global radiation of modern toads. Zenodo. (doi:10.5281/zenodo.16991998)
109. Wu D *et al*. 2025 Earth history and trait innovation drive the global radiation of modern toads. Dryad Digital Repository. (doi:10.5061/dryad.kd51c5bhv)
110. Wu D *et al*. 2025 Supplementary material from: Earth History and Trait Innovation Drive the Global Radiation of Modern Toads. Figshare. (doi:10.6084/m9.figshare.c.8054263)